Boundary conditions, entropy and the signature of random tilings

1996 J. Phys. A: Math. Gen. 29 6709

(http://iopscience.iop.org/0305-4470/29/21/007)

J. Phys. A: Math. Gen. **29** (1996) 6709–6716. Printed in the UK

Boundary conditions, entropy and the signature of random tilings

Dieter Joseph† and Michael Baake

† Institut für Theoretische Physik, Universität Tübingen, Auf der Morgenstelle 14, D-72076 Tübingen, Germany

Received 31 May 1996

Abstract. We investigate the influence of boundary conditions on the results of Monte Carlo simulations of 2D random tilings. Looking at the fluctuations in internal space we compare fixed and periodic boundaries. We find that fixed boundary conditions will lead to a different random tiling ensemble with reduced finite-size entropy density in comparison with periodic boundary conditions. As a by-product, we derive improved estimates for the elastic constants of the octagonal rhombus-tiling ensemble. Finally, we introduce a robust tool, also suitable for the analysis of experimental data, to distinguish between quasiperiodic and random-tiling models.

1. Introduction

Since the very beginning of quasicrystal research, 2D or 3D quasiperiodic tilings have been used to describe the geometric structure of these new intermetallic alloys. Even before the publication of the experimental observation [1], the standard examples for 2D and 3D ideal tilings, the Penrose tiling [2] and the Ammann–Kramer tiling [3], respectively, were known. Shortly after these publications, Elser [4] pointed out that one could relax the mathematical construction of the ideal tilings without disturbing some of their key features. Both models, ideal-quasiperiodic and random, continue to be pursued as the correct description of quasicrystalline alloys. Ideal tilings (with zero entropy density) are considered to be stabilized energetically [5] whereas in random tiling ensembles a positive entropy density is essential to minimize the free energy [6].

Focusing on the random-tiling scenario, one would like to determine the entropy density exactly. Unfortunately, until now, this has been essentially restricted to 1D. In 2D there are only very few quasicrystalline examples which have been solved exactly, such as the square–triangle tiling (12-fold) [7] and the rectangle–triangle tilings (eight-fold) [8]. In 3D there is no exact solution in sight for any example. Therefore one has to rely on numerical studies based upon Monte Carlo simulations (MC) or transfer matrix techniques.

One of the most prominent examples is the eight-fold Ammann–Beenker tiling [9], sometimes also called the octagonal rhombus tiling. In contrast to the situation of the rectangle–triangle tiling [8], it was not possible to find an exact solution for this random tiling ensemble, although it clearly has a positive entropy density. Therefore, various

† Present address: Laboratory of Atomic and Solid State Physics, Clark Hall, Cornell University, Ithaca, NY 14853-2501, USA.

0305-4470/96/216709+08$19.50

numerical studies were performed with slightly non-unique results for the entropy density†:

$$\begin{aligned} &\sigma = 0.4341(4) && \text{transfer matrix calculation (free b.c.) [10]} \\ &\sigma = 0.39(1) && \text{MC simulation (fixed b.c.) [11]} \\ &\sigma = 0.431(5) && \text{MC simulation (periodic b.c.) [12]} \\ &\sigma = 0.432(2) && \text{MC simulation (periodic b.c.) [13]} \end{aligned} \tag{1}$$

where free b.c., fixed b.c. and periodic b.c. stand for free, fixed and periodic boundary conditions, respectively. These numbers, and various other preliminary ones, have caused some confusion about the reliability of the numerical estimates. In all MC simulations, the standard hexagon flip (also called simpleton flip) approach was used to generate the random tiling ensemble starting from the ideal tiling or a periodic approximant. There exist arguments for both periodic [14] and fixed boundary conditions [15] that these flips are ergodic (i.e. each member of the corresponding ensemble can be reached by finitely many simpleton flips) wherefore one expects the simulations to give the correct entropy density. Nevertheless, a significant difference between simulations with periodic and fixed boundary conditions remains in 2D.

In a numerical simulation, the entropy density of a system is nearly the worst variable one could try to measure. One standard technique is to integrate the specific heat over temperature, which in turn can be obtained as the variance of the energy distribution of the tiling ensemble. Other methods are the histogram method and the method of entropic sampling [16], which are more efficient, but still rather computationally time consuming. So, numerical approaches to entropy require quite a lot of time, even on modern computers.

A more accessible variable is the ensemble average $\langle\overline{h^2}\rangle$ of the variance $\overline{h^2}$ of the distribution of the coarse grained internal space coordinates h_i of the ensemble members:

$$\overline{h^2} = \frac{1}{N-1}\sum_{i=1}^{N}(h_i - \overline{h})^2 \qquad \overline{h} = \frac{1}{N}\sum_{i=1}^{N} h_i. \tag{2}$$

Although it is hard to come up with a rigorous relation between the variance in internal space and the entropy density, without making crucial assumptions, it is conceivable and widely accepted that $\langle\overline{h^2}\rangle$ is the dominant term for the entropy density as a function of the system size.

In 1D this variance should be propotional to the length of the chain because the problem is equivalent to a random walk. The result is essentially the same for both boundary conditions. In 2D, the hydrodynamic approximation (see [6]) tells us that

$$\langle\overline{h^2}\rangle = \frac{1}{2\pi K_{eff}}\ln(N) + b \tag{3}$$

where K_{eff} is a combination of the elastic constants, N the number of vertices of the patch and b an additional constant due to integration of the elastic tensor in momentum space. (In 3D, the variance $\overline{h^2}$ remains bounded on the ensemble [6], so one would expect a smaller (if any) influence from boundary conditions and, in particular, power-law finite-size scaling.)

2. Influence of boundary conditions

We compared the influence of boundary conditions in the following way. For periodic b.c. we started from five successive periodic approximants with 239, 1393, 8119, 47 321

† The entropy density is given here as entropy/vertex. In the tilings under consideration, the squares fill half of the plane, so vertices/area = 1.2071.

and 275 807 vertices, respectively, and randomized them using simpleton flips. After a first thermalization period of approximately 10 000 flips per vertex we took a snapshot of the configuration at time t_1 and calculated $\overline{h^2}(N, t_1)$. Then we thermalized again and took another snapshot at t_2. At the end, we took the average over all $\overline{h^2}(N, t_i)$, $i = 1, \ldots, 5000$, as an estimate for the ensemble average. For fixed b.c. we started from circular ideal patches with zero internal strain. The vertices on the boundary of the patch were held fixed during the simulation. To take a circularly shaped patch is important because longer linear edges as in octagons can impose a tremendous effect on the entropy of the tilings even in the thermodynamic limit, as was shown for the hexagonal rhombus tiling by Elser [17].

Figure 1 shows a typical distribution of the internal coordinates after thermalization, figure 2 the variance for the different boundary conditions (bond length = 1). In both cases the hydrodynamic description is well reproduced. The logarithmic divergence is clearly

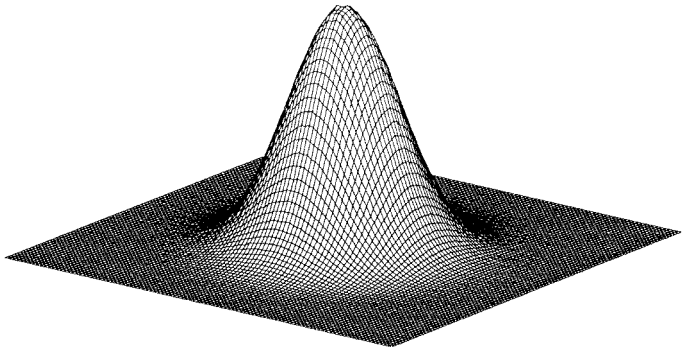

Figure 1. Distribution of internal coordinates of the randomized Ammann–Beenker tiling.

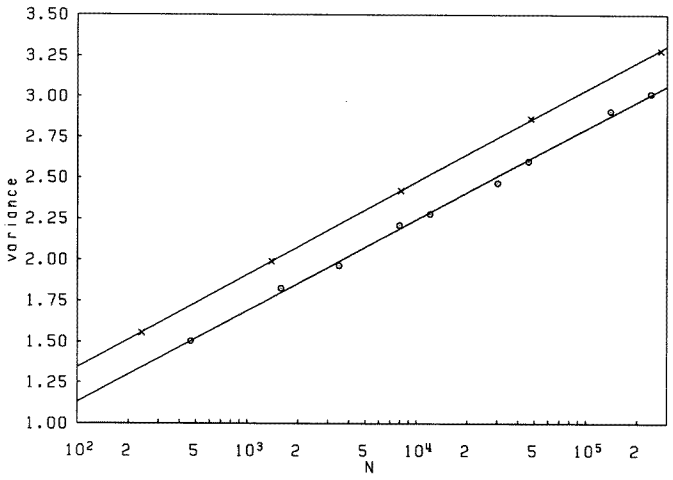

Figure 2. The (ensemble averaged) variance of the distribution of the internal coordinates of the Ammann–Beenker tiling versus the number of vertices of the patch: periodic (×) and fixed (○) boundary conditions, bond length = 1.

seen and a fit to both data sets leads to:

$$\begin{aligned}\langle\overline{h^2}\rangle_{\text{periodic b.c.}} &= 0.246(3)\ln(N) + 0.211(12)\\ \langle\overline{h^2}\rangle_{\text{fixed b.c.}} &= 0.241(6)\ln(N) + 0.020(12).\end{aligned} \tag{4}$$

The slope of both lines coincides within the fit errors. Therefore

$$\frac{\langle\overline{h^2}\rangle_{\text{periodic b.c.}}}{\langle\overline{h^2}\rangle_{\text{fixed b.c.}}} \to 1$$

in the limit $N \to \infty$. The influence of the boundary conditions on finite systems is contained in the additive constant. It is fairly large for nearly all practical patch sizes and matches the difference which occurs in the simulations of the entropy densities.

The rapid convergence (with consistent finite-size scaling behaviour) of the numerical estimates of the entropy density in the case of periodic b.c. [12, 13] leads to the conclusion that, with periodic boundary conditions, no logarithmic corrections are present in the MC calculations (see also [10] for a similar result on the transfer matrix approach).

This situation is rather different, however, for other boundary conditions where the simulations rather indicate that logarithmic corrections are present. Indeed, in view of (4), corrections of the order of $(0.191)/\ln(N)$ in the determination of the variance $\langle\overline{h^2}\rangle$ with fixed b.c. should be expected. Using $N = 10\,000$, the fixed boundary entropy calculation of [11] would therfore be expected to receive a correction of about 0.04(2) per vertex. So, both periodic b.c. and fixed b.c. lead to different finite-size random tiling ensembles, though they seem give the same entropy density in the thermodynamic limit, as long as one ensures zero strain for the boundary (otherwise this statement will not be true).

On the other hand, there is another characteristic feature of the random tiling ensemble, namely its phasonic elasticity. In the case of the octagonal tiling it is usually summarized by the elastic constants K_1, K_2 and K_3 or by the combinations

$$\begin{aligned}K_{eff} &= K_\alpha - \frac{K_\beta^2}{K_\alpha}\\ K_\alpha &= \tfrac{1}{2}(K_1 + K_2) + K_3\\ K_\beta &= \tfrac{1}{2}(K_1 - K_2).\end{aligned} \tag{5}$$

From our previous discussion, we may actually conclude that they are the same for both boundary conditions. From the transfer matrix approach [10] it was possible to calculate K_1 and K_3 with small errors. The estimation of K_2, however, was rather imprecise. Using now the much better estimate of K_{eff} from our MC simulations and combining it with the previous estimates of K_1 and K_3 of [10], one can calculate K_2 with its error reduced to one third. This way one obtains the improved estimates

$$K_1 = 0.26(1) \qquad K_2 = 0.374(40) \qquad K_3 = 0.342(4). \tag{6}$$

At this point, we have explained how the different estimates of the entropy density fit together and, as a by-product, improved the precision of the estimate of the elastic constant K_2 for the eight-fold rhombus tiling ensemble.

It is still an open question to what extent random tilings occur in nature, and how to decide whether random or quasiperiodic order is the right idealization. Let us therefore change our focus and discuss this practical issue.

3. How to distinguish random from quasiperiodic tilings

The variance of the coarse grained internal coordinates is in principle a good tool to distinguish between random tilings and ideal quasiperiodic tilings in 2D. For the former, we have a logarithmic divergence with the patch size†. For the latter, the variance is of course constant, no matter how large the patch is. Therefore, 2D is in some sense a critical dimension between the 1D (linear divergence) and the 3D (constant variance) cases. On the other hand, one has to face the practical problem that the patch sizes which can be studied by an experimentalist in HRTEM images are typically rather small, i.e. in the region of a few hundred vertices only.

Below the size of 100 vertices, the statistics is too low to say anything with certainty. One has to engage other arguments such as the total spread of the internal cloud or details of its fall-off at the shoulders, neither of which are sufficiently reliable either. Nevertheless, this variance test has been applied to experimental tilings of decagonal phases [18, 19], but without conclusive results.

In what follows, we would like to introduce a simple method to distinguish between 2D ideal quasiperiodic tilings and random tilings with a higher accuracy even if one has to face low statistics (say 500 vertices) or defects.

The inspection of the variance of the internal coordinates is motivated by the hydrodynamic approximation. The variance is the second moment of the statistical distribution of all coordinates in internal space, but the distribution itself contains a lot more information, because it encodes the correlation between the atomic position in physical space. One possibility to gain more insight is to inspect *all* statistical moments. The simplest way of doing it is to employ the Fourier transformation (FT) of the distribution of points in internal space. Let us explain why.

The FT of a distribution is the generating function of its statistical moments, i.e. they appear in the coefficients of the Taylor expansion of the FT around $k = 0$ (see [20] or any standard text on probability). Consequently, the FT of the distribution of the coordinates in internal space should be a better tool than the variance alone to distinguish between 2D ideal quasiperiodic tilings and random tilings with the same (average) symmetry. This proves true indeed, both in theoretical toy models (to be described below) and in real experiments (to be described in [21]). Especially if the statistics is poor and tiling errors are involved, one can do better this way than by using $\langle\overline{h^2}\rangle$ only.

To demonstrate our assertion, we again use the Ammann–Beenker tiling as a toy model. The *ideal* eight-fold quasiperiodic tiling has a dense and uniformly filled octagon as its acceptance domain, with simple FT. For the general argument, it is enough to approximate this octagon by a circle of the same area. The FT of a filled circle of radius R is

$$\frac{2\pi R}{k} J_1(kR) \tag{7}$$

where J_1 is the first Bessel function and k the absolute value of the wavevector. On the other hand, the internal coordinates of the *random* tiling ensemble of the Ammann–Beenker tiling approximate a Gaussian function‡ (figure 1). This is of course transformed into another Gaussian under FT.

Therefore, the FT of the internal cloud is an oscillating function in the case of the ideal tiling and approximates a Gaussian in the case of the random tiling (see figures 3 and 4).

† Here and in what follows we assume that the single member of the random tiling ensemble under consideration is typical, i.e. its individual distribution actually equals or approaches that of the ensemble average.

‡ This behaviour does *not* depend on boundary conditions.

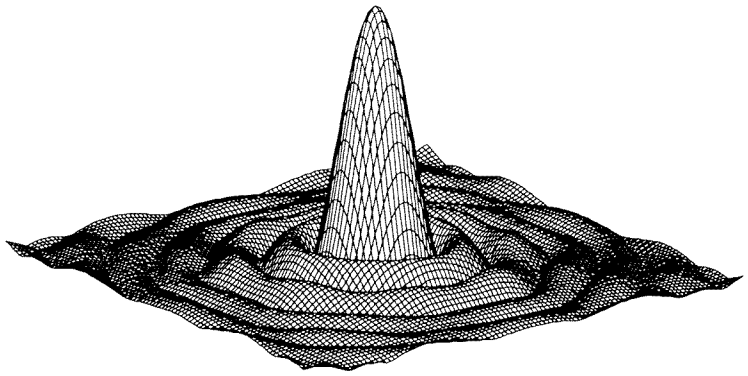

Figure 3. Absolute value of the Fourier transform of the distribution of the internal coordinates for a circular patch of 500 vertices of the ideal quasiperiodic Ammann–Beenker tiling.

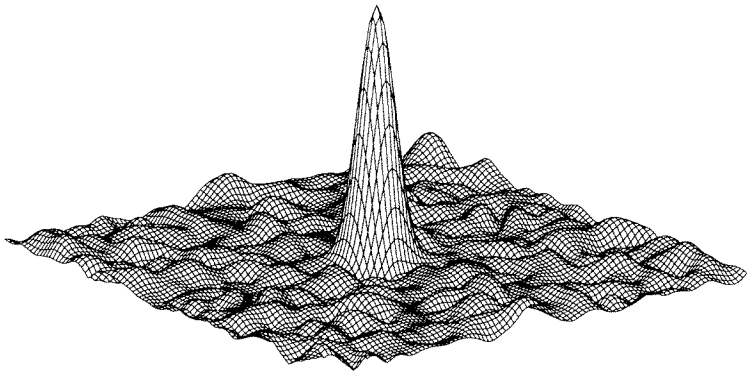

Figure 4. Absolute value of the Fourier transform of the distribution of the internal coordinates for a patch of 500 vertices of a randomized Ammann-Beenker tiling. Boundary conditions have only a minor influence on the essential features of the FT and can be neglected.

Both should behave differently even if tiling errors are involved, and the question of whether an experimental sample belongs to the class of 2D ideal quasiperiodic tilings or to the class of the random tilings should be decidable at least on the scale of the tiling. There is one (hypothetical) situation which could lead to a wrong result. If the indexed tiling is only an ideal decoration of a random tiling (supertiling) with much larger bond lengths, one would Fourier transform the convolution of the lifted decoration with a small Gaussian. This would also give an oscillating function. However, the necessary bond lengths of the supertilings are rather large. In a typical experimental situation this can often be ruled out: on the one hand, a decision between both tiling classes would make no sense if only a few supertiles would remain. On the other hand, one should find a clear signature of this supertiling in the diffraction data.

For our example we assume that a typical patch contains some 500 vertices (motivated by what can be reached in experimental HRTEM tilings). Figure 3 shows the absolute value of the discrete FT of the internal space coordinates of a quasiperiodic patch, figure 4 the corresponding one of a random patch. The behaviour described above can be clearly seen in this theoretical (error-free) system. We claim that the typical features of the FT's do

also appear in the case of real HRTEM tilings which of course contain defects of various kinds. (There, a circular integration may be employed for better statistics.) A detailed application of this approach to the investigation of HRTEM tilings of decagonal AlCoNi will be reported separately [21].

4. Conclusion

In the first part, we have presented an analysis of the influence of boundary conditions on results of MC simulations for 2D quasiperiodic tilings. We have found that fixed b.c. give rise to a significant loss in the variance of the internal coordinates and thus in the entropy density of the finite-size tiling ensemble. This is caused by logarithmic corrections. Nevertheless, one key feature of the random tiling, the elastic constants, remain unaffected and can be determined with fixed b.c. with good precision. In particular, a previous estimate of the elastic constant K_2 of the octagonal rhombus tiling could be improved in this way.

In the second part we have presented the FT of the distribution of the internal coordinates as a robust tool to distinguish between 2D ideal quasiperiodic tilings and the corresponding random tilings. We have shown the main features of the FT's in both cases and we claim that even under real experimental conditions these properties will be seen. This will be treated in a forthcoming publication [21].

Acknowledgments

It is a pleasure to thank M Schlottmann, J Hermisson, V Elser and C Henley for helpful comments, and S Ritsch and C Beeli for supplying experimental data. Financial support from the German Science Foundation (DFG) is gratefully acknowledged.

References

[1] Shechtman D, Blech I, Gratias D and Cahn J W 1984 Metallic phase with long-ranged orientational order and no translational symmetry *Phys. Rev. Lett.* **53** 1951
Ishimasa T, Nissen H-U and Fukano Y 1985 New ordered state between crystalline and amorphous in Ni–Cr particles *Phys. Rev. Lett.* **55** 511

[2] Penrose R 1974 The role of aesthetics in pure and applied mathematical research *Bull. Inst. Math. Appl.* **10** 266

[3] Kramer P and Neri R 1984 On periodic and non-periodic space fillings of E^m obtained by projection *Acta Cryst.* A **40** 580

[4] Elser V 1985 Comment on quasicrystals: a new class of ordered structures *Phys. Rev. Lett.* **54** 1730

[5] Gähler F and Jeong H-C 1995 Quasicrystalline ground states without matching-rules *J. Phys. A: Math. Gen.* **28** 1807

[6] Henley C L 1991 Random tiling models *Quasicrystals—The State of the Art* ed D P DiVincenzo and P J Steinhardt (Singapore: World Scientific) p 429

[7] Kalugin P 1994 The square–triangle random-tiling model in the thermodynamic limit *J. Phys. A: Math. Gen.* **27** 3599

[8] de Gier J and Nienhuis B 1996 Exact solution of an octagonal random tiling model *Phys. Rev. Lett.* **76** 2918

[9] Ammann R, Grünbaum B and Shepard G C 1992 Aperiodic tiles *Discr. Comput. Geom.* **8** 1
Grünbaum B and Shephard G C 1987 *Tilings and Patterns* (New York: Freeman) p 556
Beenker F P M 1982 Algebraic theory of non-periodic tilings by two simple building blocks: a square and a rhombus *TH-Report 82-WSK-04* Eindhoven
Lück R 1988 Modelling of the amorphous and quasicrystalline structures by Penrose tiling *Z. Phys. Chem., Neue Folge* **157** 843

[10] Li W, Park H and Widom M 1992 Phase diagram of a random tiling quasicrystal *J. Stat. Phys.* **66** 1

[11] Joseph D and Gähler F 1995 Specific heat and self-diffusion in quasicrystals *Aperiodic '94* ed G Chapuis and W Paciorek (Singapore: World Scientific) p 188
[12] Joseph D 1995 Specific heat and self-diffusion in quasicrystals *Quasicrystals* ed C Janot and R Mosseri (Singapore: World Scientific) p 605
[13] Gähler F 1995 Thermodynamics of random tiling quasicrystals *Quasicrystals* ed C Janot and R Mosseri (Singapore: World Scientific) p 236
[14] Gähler F 1995 Private communication
[15] Kenyon R 1995 Private communication
[16] Ferrenberg A M and Swendson R H 1988 New Monte Carlo technique for studying phase transitions *Phys. Rev. Lett.* **61** 2635
Lee J 1993 New Monte Carlo algorithm: entropic sampling *Phys. Rev. Lett.* **71** 211
[17] Elser V 1984 Solution of the dimer problem on a hexagonal lattice with boundary *J. Phys. A: Math. Gen.* **17** 1509
[18] Chen H, Burkov S E, He Y, Poon S J and Shiflet G J 1990 High-resolution microscopy study and structure modelling of the stable decagonal Al–Cu–Co quasicrystal *Phys. Rev. Lett.* **65** 72
[19] Selke H, Pohla C, Hory R and Ryder P L 1996 Hochauflösende Elektronenmikroskopie an dekagonalen Quasikristallen *DFG-Protokoll über das 6. wissenschaftliche Kolloquium im Schwerpunktprogramm Pseudosymmetrische Kristalle* 26–28 February 1996, Hünfeld
[20] Bauer H 1991 *Wahrscheinlichkeitstheorie* 4th edn (Berlin: de Gruyterr)
[21] Joseph D, Ritsch S and Beeli C 1996 How to distinguish quasiperiodic from random order *Preprint*